JOURNAL OF AIRCRAFT
Vol. 30, No. 3, May–June 1993

Limitations of Linear Theory for Sonic Boom Calculations

Christine M. Darden*
NASA Langley Research Center, Hampton, Virginia 23665

Current sonic boom minimization theories have been reviewed to emphasize the capabilities and flexibilities of the methods. Preliminary comparisons of sonic booms predicted for two Mach 3 concepts illustrate the benefits of shaping. Finally, for very simple bodies of revolution, sonic boom predictions were made using two method—a modified linear theory method and a nonlinear method—for both far-field *N*-waves and midfield signature shapes. Preliminary analysis on these simple bodies verified that current modified linear theory prediction methods become inadequate for predicting midfield signatures for Mach numbers above three. The importance of impulse in sonic boom response and the importance of three-dimensional effects which could not be simulated with the bodies of revolution will determine the validity of current modified linear theory methods in predicting midfield signatures at lower Mach numbers.

Introduction

RENEWED interest in the possible development of a high-speed civil transport (HSCT) in this country has resulted in an assessment of the technology needs and environmental concerns surrounding such a vehicle. One environmental concern which could have significant impact on the economic viability of a HSCT is the sonic boom created by supersonic overland flight. Commercial overland supersonic flight is prohibited by law in the United States. In order to examine the possibility of modifying this law, technologists must first establish an acceptability criteria and then demonstrate that this criteria can be met with an economically viable vehicle design concept. Even if overland supersonic flight does not become a reality, methods of predicting primary boom footprints, caustic levels and locations, and a statistical variability of waveforms due to atmospheric effects must be available so that any effects of sonic boom could be predicted.

Most currently used prediction methods are based on theories developed by Whitham[1] for a supersonic projectile, and by Walkden[2] who extended the analysis to include lifting bodies. These theories combined with the supersonic area rule theory developed by Hayes[3] led to the generally accepted prediction methods described in some detail in Ref. 4. Originally, it was felt that all sonic boom pressure signatures would have attained the standard *N*-wave shape when they intersected the ground. Work by McLean[5] indicated that this was not so for airplanes with extensive lifting surfaces. The "freezing" effects of the real atmosphere pointed out by Hayes[6] reinforced the idea that the signature may still retain midfield effects when it intersects the ground. A midfield signature retains effects of the airplane shape and, thus, offers shaping as a possible avenue of minimizing the sonic boom.

Using the sonic boom prediction method as a basis, the idea of midfield signature, and work by Jones[7] on the farfield minimum, Seebass and George[8,9] developed a procedure which predicted a minimizing equivalent area distribution for given flight conditions. Extensions to this procedure for the real atmosphere and nose bluntness relaxation effects are given in Refs. 10 and 11. Working inversely, the designer can develop a model whose area matches a boom-constrained distribution. This process was used to design three wing-body configurations which were experimentally tested for sonic boom levels.[12,13] Conclusions from that study indicated that the approach is valid, but that the boundary layer and wake effects must be considered in the design process. Two feasibility studies,[14,15] in which systems, passenger loads, safety, and airplane efficiency considerations were included, indicated that a low-boom aircraft was within the realm of possibility, but that further in-depth studies and tradeoffs were needed. Certain characteristic features of low-boom aircraft seemed to evolve from the studies. These features included a large wing area, long root chord, positive dihedral, twist, camber, and canards.

Propagation methods based on linearized theory become inaccurate for strong shocks where significant entropy changes occur and for high altitudes and Mach numbers where the cumulative effects of second-order terms become significant. The propagation method developed at New York University (NYU)[16] addresses many of these problems. Nonlinear terms have been retained, and altitude effects and entropy effects are included. The method of solution is the modified method of characteristics (MMOC) in which step sizes on the order of several body lengths may be taken without destroying the accuracy of the program. The program was modified to include asymmetric effects near the vertical plane of symmetry.[17] These effects are felt through derivatives in the circumferential direction which do not vanish in the vertical plane of symmetry. A further extension to this code to include shock coalescence is discussed in Ref. 18.

Ground signatures which have been used for experimental verification of modified linear theory methods have been largely of the far-field *N*-wave form since no existing aircraft have been shaped according to current minimization theories. It is suspected by some reseachers that nonlinear effects may be more prominent in predicting midfield signatures than they are for far-field *N*-waves.

Sonic boom research has escalated recently, with particular attention being given to investigating 1) minimization concepts and their validity in a real, nonquiescent atmosphere; 2) response metrics which correlate highly with perceived annoyance (i.e., initial shock, impulse, weighted loudness); 3) design of efficient, integrated aircraft systems which meet minimization constraints; and 4) the establishment of a process which may result in a definition of "acceptable" sonic boom levels.

This article briefly reviews currently accepted minimization concepts as developed by Seebass and George and other modified concepts. Flexibility within the method is discussed and the effects of varying controllable parameters are reviewed. Some of the effects of minimization discussed are for two conceptual Mach 3 configurations; one in which aerodynamic

Presented as Paper 90-0368 at the AIAA 28th Aerospace Sciences Meeting, Reno, NV, Jan. 8–11, 1990; received Feb. 22, 1990; revision received April 6, 1992; accepted for publication April 10, 1992.

*Aerospace Engineer, Vehicle Integration Branch, Advanced Vehicles Division, MS 412. Associate Fellow AIAA.

efficiency concerns dominated and a second in which sonic boom constraints dominated. Finally, the nonlinear method of Refs. 16–18 is used to predict sonic boom levels for very simple bodies-of-revolution to make a preliminary assessment of nonlinear effects on predictions and minimization methods. Other sonic boom minimization concerns such as off ground-track signatures, tail shock, and current studies to determine the proper metric are not addressed herein.

Review of Minimum Boom Concepts

An in-depth review of the minimization concepts is given in Refs. 7–11. The basic concepts of the Seebass and George minimization scheme are outlined in the upper portions of Fig. 1. Sonic boom minimization is based on an assumed form of the Whitham F function, a source distribution which at some distance from the aircraft gives the same disturbance as the aircraft. In traditional sonic boom prediction methods, the F function is defined mathematically from the equivalent area distribution of the aircraft. In minimization theories, one begins with the F function which relates directly to the resulting pressure signature. Through an inverted integral equation the F function also relates to the equivalent area distribution A_e of the defining aircraft. In its minimizing form, it has been shown[9] that the F function has a Dirac delta function at the axial location of 0. Two types of pressure signatures result with this approach to minimization, a flat top, in which overpressure is minimized, or a minimum shock, in which the initial shock is minimized. As a convenience, the slope of the F function behind the initial delta function shall be defined by η, the ratio of the slope B behind the spike, to the slope S, the dashed line ahead of the spike. For the flat-top signature, $B = 0$, thus $\eta = 0$. For a minimum shock signature, the slope B ranges from 0 to slope S, and η ranges from 0 to 1.0. The effect of varying this slope on the resulting pressure signature shape is shown in the lower right section of Fig. 1.

Depending on the design objective, each of these signatures offers advantages. Given identical conditions of Mach number, length, weight and altitude, the minimum overpressure signature results in a larger bow shock but lower total impulse, I (the integral of the positive portion of the pressure signature). As η increases, the level of the bow shock decreases, but the impulse of the signature increases. In the limit, at an η of 1.0, an N-wave with a very large bow shock results. These options are included in the minimization algorithm since the sonic boom metric which should be minimized has not been defined.

As noted previously, the minimizing form of the F function includes a Dirac delta function at the axial location of zero. This delta function corresponds to an infinite gradient at the nose of the equivalent area distribution. Aircraft designed to match these area distributions generally have extremely blunt nose shapes which result in increased drag. This result, though seemingly paradoxical, can be explained by the shock-attenuation pattern in which the shock strengths and, therefore, the drag are greatest near the aircraft. Because of special shaping and area growth, secondary shocks from the other aircraft components do not overtake and enhance the bow shock during the propagation of the wave front. The net result of this process is weaker shocks at larger distances because of attenuation, but an overall increase in drag. To allow for some flexibility in nose bluntness, the minimization algorithm was modified to incorporate a spike of finite width called the nose length.

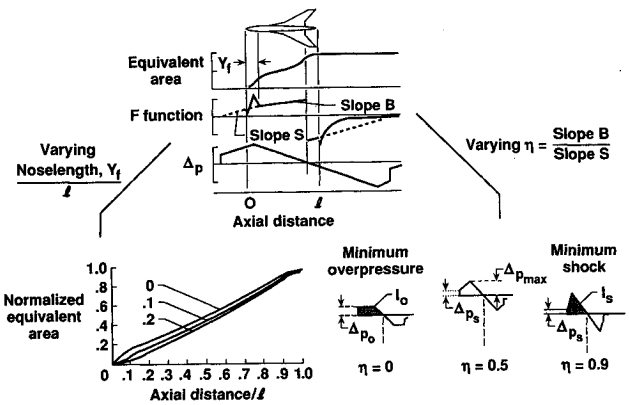

Fig. 1 Minimization concepts and parameters which may be varied.

The effect of minimizing with nose lengths y_f other than 0 is seen in the lower left section of Fig. 1. The upper equivalent area distribution results when the Dirac delta function is used. For a ratio of nose length to overall length of 0.1, the middle area distribution results. Note that a cusped region is defined in the forward part of the area distribution and that the entire curve is affected. The bow shock resulting from the middle equivalent area distribution is somewhat higher than that resulting when the delta function is used, but the use of the nose length parameter does allow flexibility between sonic boom levels and drag levels in design studies.

When using this minimization approach to achieve a given level of bow shock, use of the minimum shock signature allows one to achieve the given level with a shorter length aircraft. Conversely, use of a minimum shock signature to achieve a given bow shock allows a heavier aircraft for a given length. Other factors such as sensitivity to atmosphere and human response must also be considered.

Analysis of Two Mach 3 Concepts Using Modified Linear Theory

Concept Description

In-house studies at Langley Research Center to develop configurations for supersonic flight have resulted in two concepts which were analyzed for sonic boom trends. Planform drawings of the two concepts are shown in Fig. 2. The baseline Mach 3 configuration, the advanced supersonic transport concept (AST3), is described in more detail in Ref. 19 and is the result of a definitive systems study, with performance as the overriding constraint but with limited features included in the design process for sonic boom considerations. The Mach 3 low-boom configuration (LBM3) was designed with sonic boom as the primary consideration and factors such as range, payload, and performance considered secondarily in the initial design cycle. The configuration used for this study is a conceptual design and its use in this article is to demonstrate, even at its early stage, the effects of shaping on the sonic boom results. The long lifting length and large wing area of the LBM3 are features added to meet the target equivalent area distribution.

Analysis Methods

The equivalent area distributions of the configurations are defined using the methods described in Refs. 20–22. For the purposes of this analysis, the nacelles have not been included

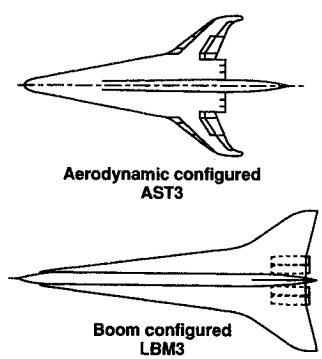

Fig. 2 Planform views of the Mach 3 baseline concept (AST3 wing area = 12,195 ft² and of the Mach 3, low-boom concept (LBM3 wing area = 13,450 ft², minimum shock signature) all linear dimensions in feet.

in the configurations. Omission of the lifting equivalent area from the nacelle integration is not expected to affect the trends which are the main purpose of this article. A comparison of the equivalent area distributions of LBM3, AST3, and the theoretical minimization curve are shown on Fig. 3 for the conditions listed. Note that the dominant feature of the low-boom equivalent area distribution is its gradual growth to achieve the maximum value at the total equivalent length. The method of Ref. 23 was used to design the camber and twist for the LBM3 wing.

Propagation of Signatures Through the Atmosphere

Using the modified linear theory propagation method described in Ref. 24, and referred to as ARAP, the equivalent area distributions shown in Fig. 3 were used to extrapolate the signatures through the atmosphere. In this analysis, it is necessary to extend the equivalent area by a factor of 2 to 3 to completely define the trailing shock. This extension can also be thought of as a simulation of the aircraft wake. ARAP includes the 1962 standard stratified atmosphere and has the capability to incorporate winds and accelerated flight, but for this comparison, a quiescent atmosphere and steady flight conditions were used.

Figure 4 shows propagation of the pressure from the idealized equivalent areas distribution as derived from the minimization algorithm for the conditions shown in the figure. Neither configuration of Fig. 3 corresponds to this area distribution. The signature near flight altitude has very large pressure levels and a portion of the forward spike is in the results. As the signature propagates through the atmosphere, more and more of the forward spike is eliminated from the signature until the signature reaches the ground where the minimum pressure is attained. Because there is no intermediate shock coalescence, full benefit of attenuation is achieved during propagation. The plot of bow shock levels during propagation (Fig. 4 inset) shows very rapid shock level changes during the initial 500 ft with the rate of change of shock level becoming almost zero until ground reflection causes a doubling of the pressure.

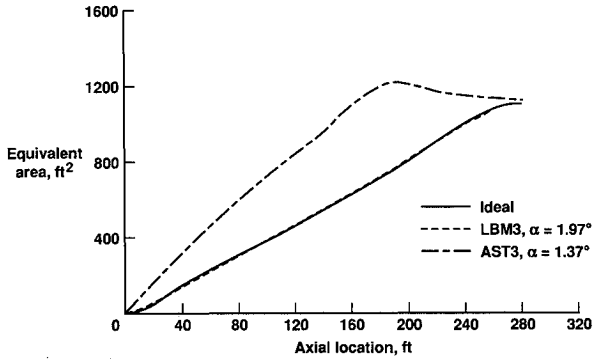

Fig. 3 Comparison of LBM3, AST3, and theoretical area distributions.

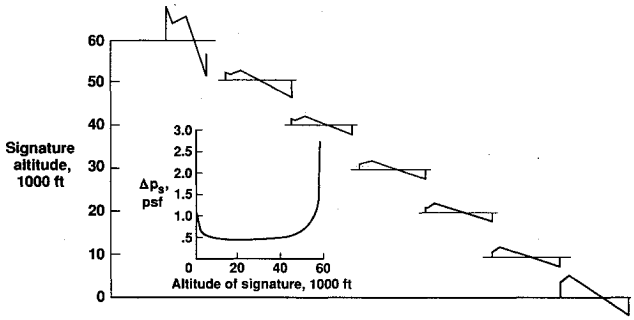

Fig. 4 Propagation of theoretical waveform through atmosphere; cruise altitude = 60,000 ft, Mach no. = 3, weight = 750,568 lb, equivalent length = 323 ft, nose length ratio = 0.1, h = 0.5, reflection factor = 1.9.

Propagation of the equivalent area for LBM3 is shown in Fig. 5. Although the exact form of the target equivalent area has not been achieved, many features of the minimization process are apparent. By comparing this figure with the propagation of the theoretical ideal signature, it could be assumed that the initial lobe of the pressure signature is a part of the initial spike of the minimizing F function. As the signature propagates through the atmosphere, more and more of this initial lobe is eliminated from the signature. For this case, the spike in the F function has not been entirely eliminated as the signature reaches the ground. Since this method of minimization requires a precise prediction of the minimum point, some indication of its sensitivity to other atmospheric effects is needed.

Rather than a linear pressure rise behind the initial lobe such as that in the theoretical signature, the pressure rise is experienced through the two shocks. Notice, however, that the coalescence of these shocks has been suppressed until the signature reaches ground level, a goal in minimization. The relationship between the equivalent area distribution and the resulting pressure signatures is through the second derivative of the area. This relationship implies that in the aircraft design process, an attempt must be made to match not only the equivalent areas but also the derivatives of the areas. Two methods[25,26] have recently been developed at NASA which can be used in the final design stages to produce this match more closely. Both methods are based on making all final area adjustments to the fuselage of the configuration.

Propagation of the signature for AST3, the aerodynamic concept, is shown in Fig. 6. Where the signatures shown in Figs. 4 and 5 were for altitudes ranging from 60,000 ft to the ground, changes in this signature occurred so rapidly that only 7000 ft near the aircraft are shown. Attenuation reduces the bow shock level very rapidly as with signatures in the previous two figures. This signature, however, produces a coalescence of the bow shock and the embedded shock between 53,000–54,000 ft. The inset plot of overpressure levels vs signature altitude shows that when this coalescence occurs, the bow shock again increases from about 1.2 to about 1.65 psf. Thus

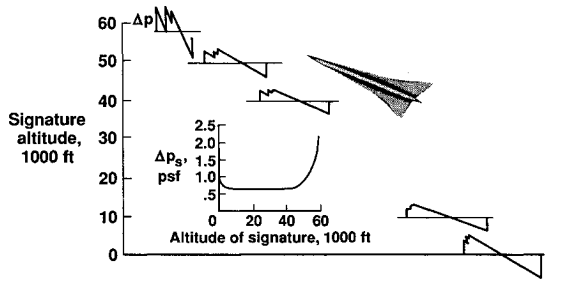

Fig. 5 Propagation of signature of LBM3 configuration: cruise altitude = 60,000 ft, Mach no. = 3, angle of attack = 1.97 deg, weight = 750,568 lb, reflection factor = 1.9.

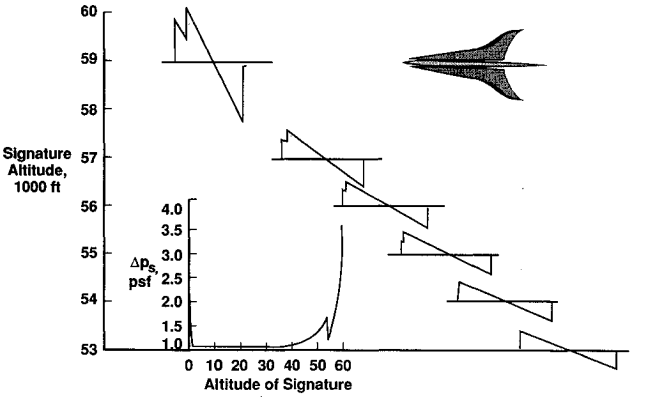

Fig. 6 Propagation of AST3 signature through atmosphere; cruise altitude = 60,000 ft, Mach no. = 3, weight = 752,853 lb, equivalent length = 280 ft, angle of attack = 1 deg, reflection factor = 1.9.

attenuation must start again in a region of the atmosphere where attenuation rates have slowed considerably. The bow shock level only attenuates to 1.1 psf before it reaches the ground and is again magnified to roughly 2.2 psf due to ground reflection.

A comparison of the propagation pattern of these three equivalent area distributions illustrates that if one can maintain midfield effects over a certain distance then those midfield effects will generally persist to the ground because of the freezing effects of the atmosphere.

Comparison of Bow Shock Levels

The effectiveness of low-boom shaping and some indication of its sensitivity to Mach number and altitude variation can be seen in Figs. 7 and 8. In Fig. 7, a comparison of bow shock overpressures for the AST3 baseline and the LBM3 low-boom concept are shown. The inset pressure signatures shown are to the same scale and indicate how the ground signature changes as the aircraft cruises at different altitudes. Note that for both configurations, there is a decrease in overpressure as altitude increases. The discontinuity in overpressure in both curves occurs when the signature changes from a midfield, multishock signature, to a classic N-wave. Two benefits of the LBM3 are obvious: 1) its bow shock overpressure level is substantially lower than that of the AST3 for the entire altitude range shown, and 2) its transition to an N-wave is delayed to a higher altitude. In the midfield region of both signatures, the bow shock of the AST3 is about 45% higher than the low boom. In the region around 68,000-ft alt where the AST3 signature is an N-wave and the LBM3 signature is still midfield, the AST3 has a boom which is 65% higher than the low boom. After both signatures have transitioned to N-waves, the benefit of the low boom shaping practically disappears. The design cruise conditions for the LBM3 configuration are Mach 3 at 65,000 ft.

The variation of bow shock overpressure with Mach number for the same two concepts is shown in Fig. 8. Generally for the midfield signatures, there is a slight increase in bow shock overpressure with increasing Mach number. For the far-field

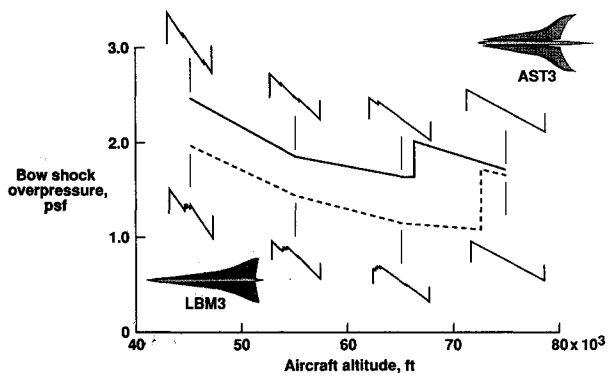

Fig. 7 Ground overpressure as a function of aircraft altitude; Mach no. = 3, weight = 600,000 lb.

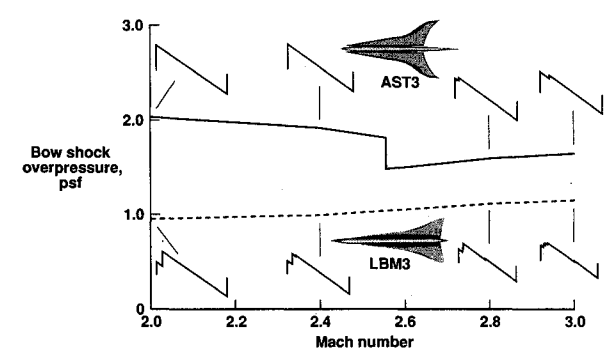

Fig. 8 Ground overpressure as a function of Mach number; aircraft altitude = 65,000 ft, weight = 600,000 lb.

N-wave, as seen for the AST3 at Mach 2–2.4, there is a slight decrease in overpressure with Mach number. Again the benefit of low-boom shaping on the bow shock overpressure is shown for the entire Mach range shown. Similar calculations of perceived loudness in decibels (PLdB) showed the same trends with altitude and Mach number, but are not shown here.

The benefit of shaping in lowering bow shock overpressure is clearly shown in these figures. It is also shown that the benefits are maitntained to a substantial degree at off-design Mach numbers and to a lesser degree at off-design altitudes.

Predictions Using Modified Method of Characteristics

The remainder of this article discusses results of preliminary comparisons of sonic boom predictions made using the standard modified linear theory methods and the nonlinear MMOC described in Refs. 16–18. The MMOC is a propagation method and requires flowfield data on a cylindrical surface at approximately one body length from the longitudinal axis as input. This data can be supplied either from experimental data or by use of computational flowfield methods. To employ the MMOC in an axisymmetric mode, the initial data must include, axial location x, radial location r, flow angularity θ, Mach number M, and entropy S, in the plane of symmetry beneath the flight path. In addition, the strength of the bow shock and the location and strengths of any embedded shocks must be given. For asymmetric cases, cross derivatives of the flow variables are also required.

Because there is no experimental data with which to directly validate the MMOC method, validation will be accomplished indirectly by comparison with codes which have been validated. The method of Ref. 24 (ARAP) has been previously compared with flight data and shown to be valid for far-field N-waves at moderate Mach numbers. A comparison taken from Ref. 4 is shown on the top right of Fig. 9. A second comparison at a much higher Mach number (lower right), but at a closer radial distance, shows that though the level of the bow shock is nearly correct, the length of the signature is poorly predicted. Recall that the method of Ref. 24 is initialized with geometry and the F-function approach is used to predict the final signature. To initialize MMOC, flowfield data is needed at distances so close to the longitudinal axis of the body, that ARAP is not valid. The method of Ref. 27 [modified uniform atmosphere method (MUAM)] was chosen to generate data for initializing MMOC calculations. Near-field comparisons of MUAM predictions and experimental data for two bodies-of-revolution are also shown in Fig. 9. These results indicate that MUAM predictions are valid in the near-field and that bow shock levels predicted by ARAP at large distances are generally valid.

Based on the previous discussion, the MUAM code was used to generate flowfield data in the vicinity of the body-of-revolution shown in Fig. 10. Predictions using MUAM for

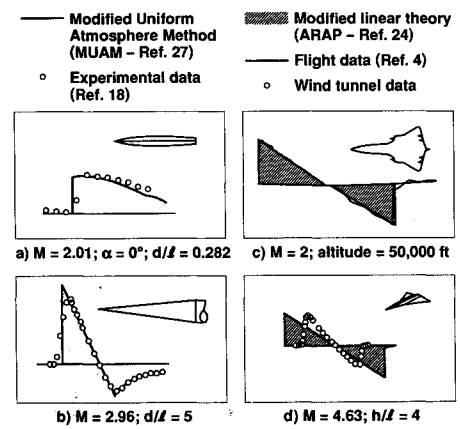

Fig. 9 Comparison of theoretical predictions and experimental data from Refs. 27 and 24.

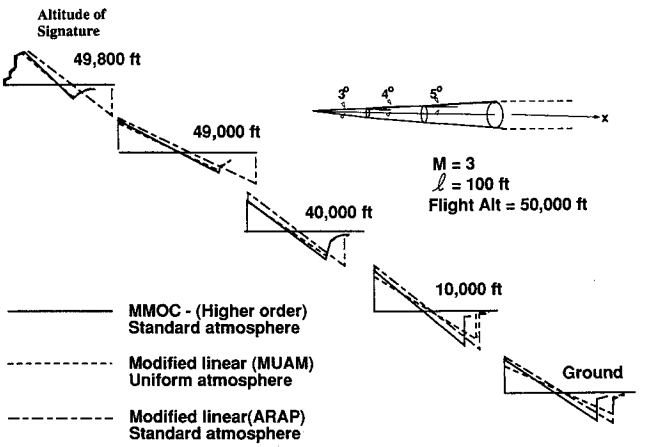

Fig. 10 Comparison of signature propagation; Mach no. = 3, angle of attack = 0 deg, length = 100 ft, cruise altitude = 50,000 ft.

this 3-4-5-deg cone of revolution are shown from a distance of two body lengths to the ground with the short dashed line. The solid lines represent MMOC predictions, and the long-short dashed line the results of ARAP. As previously mentioned, the results from MUAM at one body length have been used to initialize MMOC.

The results shown are for this cone flying at a speed of Mach 3 and at 0-deg angle of attack at 50,000 ft. Changes occur very rapidly in the pressure signatures and all signatures have become *N*-waves within the first 1000 ft. Note at this Mach number and angle of attack, the MMOC and MUAM signatures remain very near each other through 100 body lengths. At ground level, the bow shock predictions of the MMOC and the ARAP are near each other, although the MMOC signature is predicted to be significantly shorter.

These results indicate that at this Mach number and for these simple axisymmetric bodies, the results predicted by ARAP are of sufficient accuracy to predict the bow shock of the *N*-wave signatures, although the impulse of the signature predicted for the cone at 0-deg angle of attack by MMOC would be somewhat less than that predicted by ARAP.

The signatures of these cones changed very rapidly into *N*-waves, as did that of the AST3 configuration at Mach 3. To investigate the differences in propagation results for a low-boom shaped configuration, the equivalent area distribution as described by the minimization algorithm was converted into a body-of-revolution and the method of Ref. 27 was again used to generate the input needed for MMOC. Results of this exercise for two different flight conditions are shown in Figs. 11 and 12. Shown for comparison with the MMOC results, are results predicted by the minimization algorithm[11] SEEB, a method equivalent to ARAP. A discussion of some of the limitations of using a body-of-revolution to represent a three-dimensional lifting body with nacelles is found in Ref. 28.

Figure 11 shows as a dashed line the flat-top pressure signature predicted using SEEB. Results for the body-of-revolution derived using the resulting equivalent area distribution and extrapolated in MMOC are shown as the solid line. While midfield effects are still evident in the ground signature, it does not display the flat-top as predicted by the modified linear methods. The bow shock predicted by SEEB is 0.9867 psf and that by MMOC is 1.058 psf. MMOC also predicts a steady decline in pressure level to approximately 0.90 psf before the expansion region. At this Mach number, the comparisons seem to indicate that use of the modified linear theory methods are adequate for preliminary design work and studies, especially if the impulse of the signature does not have a high correlation with disturbance. If impulse is significant, then the lower impulse predicted by the MMOC, 0.10579 lb-s/ft^2 as compared to 0.1356 lb-s/ft^2 for SEEB, could be a significant factor at Mach 2.7.

Figure 12 shows the same results for a body-of-revolution from equivalent area which has been optimized at the conditions shown. While SEEB indicates a bow shock of 0.99 psf and a following pressure rise to a level of 1.7 psf which results in an impulse of 0.2564 lb-s/ft^2, MMOC predicts a bow shock level of 1.23 psf, a following pressure rise to 1.30 psf and an impulse of 0.18486 lb-s/ft^2. A comparison of these two signatures indicates that the difference in the bow shock level is significant and the difference in the impulse levels is also significant. This would imply that at Mach 3.5 modified linear theory methods may not be sufficient for predicting minimized, or midfield-shaped signatures. This difficulty with linear theory methods has been reported previously in Ref. 29.

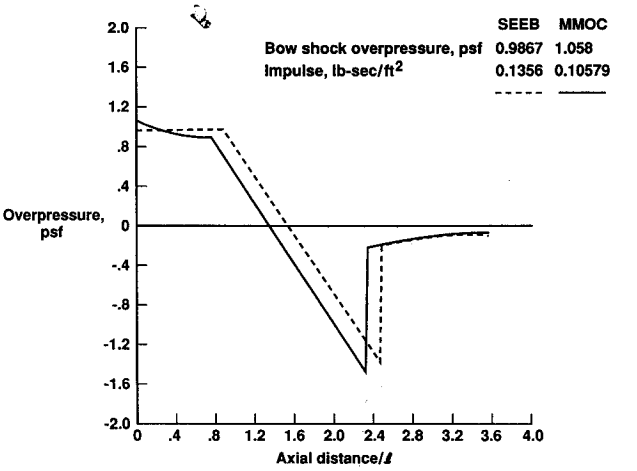

Fig. 11 Comparison of theoretical waveform propagation using modified linear theory and MMOC; Mach no. = 2.7, cruise altitude = 60,000 ft, weight = 600,000 lb, nose length ratio = 0.08, equivalent length = 310 ft, ratio of rear shock to front shock = 1.2.

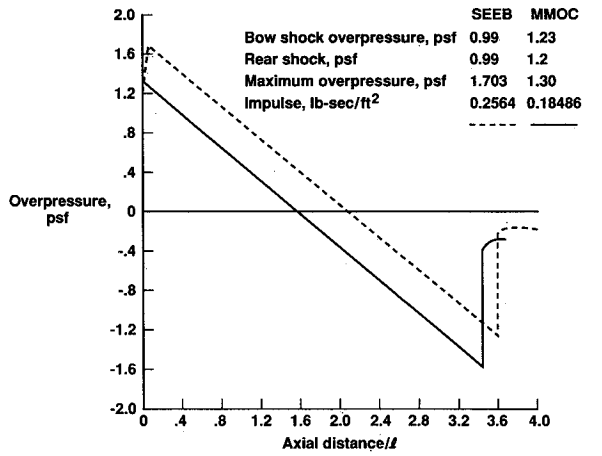

Fig. 12 Comparison of theoretical waveform propagation using modified linear theory and MMOC; Mach no. = 3.5, cruise altitude = 70,000 ft, weight = 650,000 lb, equivalent length = 310 ft, nose length ratio = 0.07, ratio of rear shock to front shock = 1.2.

Conclusion

Modified linear theory analysis of two Mach 3 configurations and analysis of a body-of-revolution using a higher order code and modified linear theory indicate the following:

1) Configuration shaping for low boom does provide benefit in lowering its bow shock overpressure, but signature variations with atmospheric conditions must be monitored.

2) Modified linear theory prediction methods become inadequate for predicting midfield signatures for Mach numbers near 3 and above.

3) The importance of impulse in sonic boom disturbance and the importance of three-dimensional effects which could not be simulated with the bodies-of-revolution will determine the validity of current modified linear theory methods in predicting midfield signatures at lower Mach numbers.

4) Further study using flowfield results or experimental data from a fully three-dimensional configuration with nacelles and other components is required.

References

[1]Whitham, G. B., "The Flow Pattern of a Supersonic Projectile," *Communication Pure and Applied Mathematics*, Vol. V, No. 3, 1952, pp. 301–348.

[2]Walkden, F., "The Shock Pattern of a Wing-Body Combination, Far from the Flight Path," *Aeronautical Quarterly*, Vol. IX, Pt. 2, May 1958, pp. 164–194.

[3]Hayes, W. D., "Linearized Supersonic Flow," North American Aviation, Rept. AL-222, June 18, 1947.

[4]Carlson, H. W., and Maglieri, D. J., "Review of Sonic-Boom Generation Theory and Prediction Methods," *Journal of Acoustical Society of America*, Vol. 51, No. 2, Pt. 3, 1972, pp. 675–685.

[5]McLean, F. E., "Some Nonasymptotic Effects on the Sonic Boom of Large Airplanes," NASA TN D-2877, 1965.

[6]Hayes, W. D., "Brief Review of Basic Theory," *Sonic Boom Research*, edited by A. R. Seebass, NASA SP-147, 1967, pp. 3–7.

[7]Jones, L. B., "Lower Bounds for Sonic Bangs in the Far Field," *Aeronautical Quarterly*, Vol. XVIII, Pt. 1, Feb. 1967, pp. 1–21.

[8]Seebass, R., "Sonic Boom Theory," *Journal of Aircraft*, Vol. 6, No. 3, 1969, pp. 177–184.

[9]Seebass, R., and George, A. R., "Sonic-Boom Minimization," *Journal of Acoustical Society of America*, Vol. 51, No. 2, Pt. 3, 1972, pp. 686–694.

[10]Darden, C. M., "Minimization of Sonic-Boom Parameters in Real and Isothermal Atmospheres" NASA TN D-7842, March 1975.

[11]Darden, C. M., "Sonic-Boom Minimization with Nose-Bluntness Relaxation," NASA TP-1348, Jan. 1979.

[12]Mack, R. J., and Darden, C. M., "Wind-Tunnel Investigation of the Validity of a Sonic-Boom Minimization Concept," NASA TP-1421, Oct. 1979.

[13]Mack, R. J., and Darden, C. M., "Some Effects of Applying Sonic Boom Minimization to Supersonic Cruise Aircraft Design," *Journal of Aircraft*, Vol. 17, No. 3, 1980, pp. 182–186.

[14]Sigalla, A., Runyan, L. J., and Kane, E. J., "The Overland Supersonic Transport with Low Sonic Boom—A Feasibility Study," *Acta Aeronautica*, Vol. 4, Nos. 1 and 2, 1977, pp. 163–179.

[15]Carlson, H. W., Barger, R. L., and Mack, R. J., "Application of Sonic-Boom Minimization Concepts in Supersonic Transport Design," NASA TN D-7218, June 1973.

[16]Ferri, A., Siclari, M., and Ting. L., "Sonic Boom Analysis for High Altitude Flight at High Mach Numbers," AIAA Paper 73-1034, Oct. 1973.

[17]Ferri, A., Ting, L., and Lo, R. W., "Nonlinear Sonic-Boom Propagation Including the Asymmetric Effects," *AIAA Journal*, Vol. 15, No. 5, 1977, pp. 653–658.

[18]Darden, C. M., "An Analysis of Shock Coalescence Including Three Dimensional Effects with Application to Sonic Boom Extrapolation," NASA TP-2214, Jan. 1984.

[19]Robins, A. W., Dollyhigh, S. M., Beissner, F. L., Jr., Geiselhart, K., Martin, G. L., Shields, E. W., Swanson, E. E., Coen, P.G., and Morris, S. J., Jr., "Concept Development of a Mach 3.0 High-Speed Civil Transport," NASA TM 4058, Sept. 1988.

[20]Harris, R. V., Jr., "A Numerical Technique for Analysis of Wave Drag at Lifting Conditions," NASA TN D-3586, Nov. 1966.

[21]Carlson, H. W., and Mack, R. J., "Estimation of Wing Nonlinear Aerodynamic Characteristics at Supersonic Speeds," NASA TP-1718, March 1980.

[22]Mack, R. J., "A Numerical Method for Evaluation and Utilization of Supersonic Nacelle-Wing Interference," NASA TN D-5057, March 1969.

[23]Carlson, H. W., and Miller, D. S., "Numerical Methods for the Design and Analysis of Wings at Supersonic Speeds," NASA TN D-7713, Dec. 1974.

[24]Hayes, W. D., Haefeli, R. C., and Kulsrud, H. E., "Sonic Boom Propagation in a Stratified Atmosphere, with Computer Program," NASA CR-1299, April 1969.

[25]Mack, R. J., and Needleman, K. E., "A Semi-Empirical Method for Obtaining Fuselage Normal Areas from Fuselage Mach Sliced Areas," NASA TM-4228, Dec. 1990.

[26]Barger, R. L., and Adams, M. S., "Fuselage Design for a Specified Mach Sliced Area Distribution," NASA TP-2975, Feb. 1990.

[27]Mack, R. J., "An Improved Method for Calculating Supersonic Pressure Fields About Bodies of Revolution," NASA TN D-6508, Oct. 1971.

[28]Carlson, H. W., McLean, F. E., and Shrout, B. L., "A Wind-Tunnel Study of Sonic-Boom Characteristics for Basic and Modified Models of a Supersonic Transport Configuration," NASA TM X-1236, May 1966.

[29]Morris, O., "Experimental Studies of Sonic Boom Phenomena at High Supersonic Mach Numbers," *Proceedings of Third Conference on Sonic Boom Research*, NASA SP-255, 1970, p. 193.